A “glympse” into neurodegeneration: diffusion MRI and cerebrospinal fluid AQP4 for the assessment of glymphatic system in Alzheimer’s disease and other dementias

Luca Sacchi[1], Federico D’Agata[2], Corrado Campisi[2], Marina Arcaro[3], Tiziana Carandini[3], Balázs Örzsik[4], Vera Pacoova Dal Maschio[2,5], Chiara Fenoglio[1], Anna Margherita Pietroboni[3], Laura Ghezzi[1], Maria Serpente[3], Manuela Pintus[3], Giorgio Conte[3,6], Fabio Triulzi[3,6], Leonardo Lopiano[2,5], Daniela Galimberti[1], Mara Cercignani[7], Marco Bozzali[2,5] and Andrea Arighi[3]

[1]Department of Biomedical, Surgical and Dental Sciences, University of Milan, Milan, Italy
[2]Department of Neurosciences “Rita Levi Montalcini”, University of Turin, Turin, Italy
[3]Fondazione IRCCS Ca' Granda, Ospedale Maggiore Policlinico, Milan, Italy
[4]Department of Radiology, Leiden University Medical Center, Leiden, The Netherlands
[5]Neurology 2 Unit, A.O.U. Città della Salute e della Scienza di Torino, Turin, Italy
[6]Department of Pathophysiology and Transplantation, University of Milan, Milan, Italy
[7]Brain Research Imaging Centre, Cardiff University, Cardiff, United Kingdom

***Corresponding Author:**

Luca Sacchi

Fondazione IRCCS Ca' Granda Ospedale Policlinico

Via F. Sforza 35, 20122 Milan, Italy

+39025503870

Email: luca.sacchi1@unimi.it

ORCID: 0000-0002-3929-9009

Abstract word count: 426
Text word count: 5333

Key Words: glymphatic system, aquaporin 4, brain perivascular spaces, diffusion magnetic resonance imaging, cerebrospinal fluid, Alzheimer disease, neurodegenerative disease, dementia

Key points:

- Diffusion MRI and the quantification of AQP4 in the cerebrospinal fluid may serve as indirect biomarkers of glymphatic activity in vivo
- Neurodegeneration is associated with diffuse changes of MRI parameters of glymphatic activity and AQP4 levels in the CSF
- Changes of glymphatic biomarkers are partly depending on disease stage and measures of structural brain damage

Declarations

Availability of data and materials: the datasets used in this study are available from the corresponding author upon reasonable request.

Authors' contributions: LS and AA designed the study, analyzed and interpreted the data. LS drafted the manuscript. AA, TC, AMP, LG, FD, CC and MP contributed to the analysis and interpretation of the data. MA, MS and CF performed CSF analyses. MB, MC, BO, VP, FD and CC helped in the analysis of MRI data. FT and GC acquired MRI data. AA, MB, LL and DG drafted and revised the manuscript for intellectual content. All authors read and approved the final manuscript.

Statement on ethics approval: all procedures performed in studies involving human participants were in accordance with the ethical standards of the institutional and/or national research committee and with the 1964 Helsinki declaration and its later amendments or comparable ethical standards.

Informed consent: informed consent was obtained from all individual participants included in the study.

Competing interests: the authors declare that they have no competing interests.

Funding and Acknowledgements: this work was supported by grants from the Italian Ministry of Health (Ricerca Corrente). MS. is supported by the Italian Ministry of Health, grant GR-2019-12369100.

Abstract

Background: The glymphatic system (GS) is a whole-brain perivascular network, consisting of three compartments: the periarterial and perivenous spaces and the interposed brain parenchyma. GS dysfunction has been implicated in neurodegenerative diseases, particularly Alzheimer's disease (AD). So far, comprehensive research on GS in humans has been limited by the absence of easily accessible biomarkers. Recently, promising non-invasive methods based on magnetic resonance imaging (MRI) along with aquaporin-4 (AQP4) quantification in the cerebrospinal fluid (CSF) were introduced for an indirect assessment of each of the three GS compartments.

Methods: we recruited 111 consecutive subjects presenting with symptoms suggestive of degenerative cognitive decline, who underwent 3T MRI scanning including multi-shell diffusion-weighted images. Forty-nine out of 111 also underwent CSF examination with quantification of CSF-AQP4. CSF-AQP4 levels and MRI measures – including perivascular spaces (PVS) counts and volume fraction (PVSVF), white matter free water fraction (FW-WM) and mean kurtosis (MK-WM), diffusion tensor imaging analysis along the perivascular spaces (DTI-ALPS) (mean, left and right) – were compared among patients with AD (n=47) and other neurodegenerative diseases (nAD=24), patients with stable mild cognitive impairment (MCI=17) and cognitively unimpaired (CU=23) elderly people. Two runs of analysis were conducted, the first including all patients; the second after dividing both nAD and AD patients into two subgroups based on grey matter atrophy as a proxy of disease stage. Age, sex, years of education and scanning time were included as confounding factors in the analyses.

Results: considering the whole cohort, patients with AD showed significantly higher levels of CSF-AQP4 (exp(b)=2.05, p=0.005) and FW-WM FW-WM (exp(b)=1.06, p=0.043) than CU. AQP4 levels were also significantly higher in nAD in respect to CU (exp(b)=2.98, p<0.001).
CSF-AQP4 and FW-WM were significantly higher in both less atrophic AD (exp(b)=2.20, p=0.006; exp(b)=1.08, p=0.019, respectively) and nAD patients (exp(b)=2.66, p=0.002; exp(b)=1.10, p=0.019, respectively) compared to CU subjects.
Higher total (exp(b)=1.59, p=0.013) and centrum semiovale PVS counts (exp(b)=1.89, p=0.016), total (exp(b)=1.50, p=0.036) and WM PVSVF (exp(b)=1.89, p=0.005) together with lower MK-WM (exp(b)=0.94, p=0.006), mean and left ALPS (exp(b)=0.91, p=0.043; exp(b)=0.88, p=0.010 respectively) were observed in more atrophic AD patients in respect to CU. In addition, more atrophic nAD patients exhibited higher levels of AQP4 (exp(b)=3.39, p=0.002) than CU.

Discussion: our results indicate significant changes in putative MRI biomarkers of GS and CSF-AQP4 levels in AD and in other neurodegenerative dementias, suggesting a close interaction between glymphatic dysfunction and neurodegeneration, particularly in the case of AD. However, the usefulness of some of these biomarkers as indirect and standalone indices of glymphatic activity may be hindered by their dependence on disease stage and structural brain damage.

Main text

1. Introduction

The glymphatic system (GS) is a perivascular network which plays a fundamental role in waste removal from the brain. GS has a three-compartment organization, in which subarachnoid cerebrospinal fluid (CSF) enters the brain's interstitium from the periarterial spaces facilitated by aquaporin-4 (AQP4), mixes with the interstitial fluid (ISF) and waste solutes – including pathological proteins like amyloid-β (Aβ) and tau – and is then drained out of the brain by perivenous efflux routes into meningeal and cervical lymphatics[1–3].

Gold-standard in-vivo evaluation tools for GS require intrathecal[4,5] or intravenous[6] administration of gadolinium based contrast agents (GBCA) or radioactive tracers[7], whose relative invasiveness has limited comprehensive research in humans. Recently, there has been a growing effort to identify less invasive and more easily accessible biomarkers of GS function.

Promising magnetic resonance imaging (MRI)-based techniques have been introduced for an indirect evaluation of glymphatic activity. These include enlarged perivascular spaces (PVS) quantification and diffusion-based techniques.

PVS are fluid-filled compartments enveloping brain penetrating arterioles and are considered as a major component of the GS. PVS are known to become enlarged in many clinical conditions. Enlarged PVS in the basal ganglia (BG) are primarily associated with aging and hypertension[8,9], while enlarged PVS in the centrum semiovale (CSO) have been associated with amyloid deposition[10–12] and neurodegeneration. Indeed, impaired glymphatic clearance may limit effective removal of pathological proteins from the brain and clog up the system upstream, leading to further reduction of perivascular drainage, PVS enlargement and ultimately neurodegeneration. Once dilated, PVS can be quantified on MRI using visual scoring scales[13,14] or, more accurately, with a wide range of segmentation techniques, spanning from classical image processing approaches to deep neural network modelling[15–18].

Diffusion-weighted (DW)-MRI enables the evaluation of brain microstructure by probing microscopic diffusivity of water molecules[19]. Most commonly, diffusion-related parameters are derived using the diffusion tensor (DT) model (i.e DT-imaging: DTI)[20]. The DTI-based analysis along the perivascular spaces (ALPS) was developed to evaluate the diffusivity along the PVS of the deep medullary veins, which is regarded as a proxy measure of glymphatic clearance[21]. The usefulness of ALPS index as a non-invasive biomarker of GS function was supported by a recent comparison with data obtained by intrathecal GBCA tracers[5].

DT is a widely acknowledged model that, however, suffers from several limitations[22]. To overcome these limitations, a free-water (FW) correction algorithm was developed to remove

the contribution of extracellular FW to DTI-derived metrics[23]. Elevated FW in the white matter (WM) has been observed in patients with AD, suggesting impaired fluid drainage likely attributable to glymphatic dysfunction[24–27], and the FW index has been proposed as a standalone biomarker of AD-related pathology[24,19,28,26].

Diffusion-kurtosis imaging (DKI) is a higher order diffusion model that represents another evolution of the DTI, accounting for non-gaussian diffusion of water molecules[29,30]. Metrics derived from DKI, particularly mean kurtosis (MK), have been suggested as putative indices of glymphatic activity[31]. In fact, it was recently shown that the expansion of interstitial space associated with sleep results in a reduction of diffusion non-Gaussianity and hence of diffusion kurtosis.

Besides MRI-based markers, recent data suggest a potential utility of quantifying CSF-AQP4 levels for the detection of glymphatic dysregulation[32]. AQP4 is a water channel densely expressed on the perivascular side of astrocytes lining PVS. Its polarized localization is essential for the rapid influx of fluid from periarterial spaces into the brain parenchyma. In neurodegeneration due to AD pathology, AQP4 is known to be over-expressed and mislocalized away from astrocytic endfeet processes[33,34], possibly impairing glymphatic clearance of waste solutes and pathological proteins[35,36]. Consistent with this, levels of AQP4 were found to be increased in the CSF of patients affected by neurodegenerative dementia, particularly AD[37,32]. Moreover, preliminary data suggest an association between CSF levels of AQP4, tau protein levels[32] and enlarged PVS burden, particularly in the CSO[38].

Different biomarkers may preferably mirror alterations in one the three compartments of the GS. Although the precise anatomical substrate of enlarged PVS is still under debate, the overall evidence suggests that they represent periarterial spaces[39]. Given the close spatial and functional relationship between PVS and AQP4, the latter might primarily represent a marker of periarterial pathophysiological mechanisms. Nonetheless, AQP4 is also expressed on brain capillaries and veins[3], and thus might potentially indicate more widespread aspects of GS dysfunction. FW and MK mainly mirror changes in parenchymal microstructure and fluid content, providing information about ISF, while the DTI-ALPS index is a measure of the diffusivity along the PVS around the deep medullary veins. Together, all these biomarkers may enable an indirect evaluation of the whole GS in vivo.

Against this background, the principal aim of this study was to evaluate the changes of these putative biomarkers of GS function in patients with neurodegenerative diseases, particularly AD, and with stable mild cognitive impairment (MCI) in respect to healthy elderly people. The secondary aims were to evaluate the reciprocal correlations among GS biomarkers and the correlations between these parameters and established markers of AD pathology and neurodegeneration and cognitive scores.

2. Materials and methods

2.1 Study participants

For this study, we prospectively enrolled a cohort of subjects from those referred to the Neurodegenerative Diseases Unit of the Fondazione IRCCS Ca' Granda Ospedale Maggiore Policlinico in Milan (Italy) in suspicion of dementia, over a 12-month period. In addition to the assessments needed to formulate (or exclude) a specific diagnosis of dementia, recruited participants were required to undergo an additional 10-mins long acquisition (i.e., multi-shell DW-MRI) at the end of their MRI clinical scan, and to give permission to use their clinical data (in anonymous form) for research purposes. Whenever a CSF examination was clinically appropriate, subjects were given the option to agree to the collection of an extra CSF sample for quantification of AQP4 levels.

At baseline, in all subjects the diagnostic work-up included past medical history; general and neurological examination; neuropsychological assessment; MRI scanning; and, when appropriate, CSF examination.

All recruited patients were clinically followed-up every 6 months for at least 1 year, and reclassified as suffering from a progressive neurodegenerative disease (AD or non-AD type), or a non-degenerative condition (stable MCI) if they were discharged with no evidence of neurodegeneration and did not show cognitive deterioration at follow-up. Cognitively unimpaired (CU) individuals presented with subjective memory complaints and underwent an extensive diagnostic work-up, which did not provide any evidence for cognitive impairment or an ongoing neurodegenerative condition.

Exclusion criteria for enrolment in the study were: a) previous history of major psychiatric disorders; b) MRI evidence of remarkable vascular pathology, cerebral amyloid angiopathy (CAA), or intracranial space-occupying lesions; c) coarse movement artifacts on MRI scans.

The study involving human participants was reviewed and approved by the Local Ethics Committee (Comitato Etico Area 2 Milano, approval N 859_2021, date 14.09.2021). All participants and their legal guardians (when appropriate) were required to provide written informed consent before entering the study.

2.2 MRI acquisition

MRI data were acquired on a Philips Achieva dStream 3T scanner (Eindhoven, Netherlands) in a single scanning session. All the subjects underwent the same acquisition protocol, which included:

1) A volumetric high-resolution T1-weighted magnetization prepared gradient recalled echo images (MPRAGE; TE=3.81 ms; TR=8.27 ms; flip angle=8°; matrix=240x240x180; slice thickness= 1 mm);
2) A volumetric fast fluid-attenuated inversion recovery (FLAIR: TE=300 ms; TR=5000 ms; TI=1700 ms; echo-train-length=182, flip angle=90°; matrix=240x240x180; slice thickness=1 mm; slice spacing= 1 mm)
3) A multi-shell DW-MRI scan (TE=85 ms, TR=8400, b values=1000/2000 smm-2, number of diffusion directions=32/32, FoV=240x240 mm2, matrix=96x96, number of slices=60; slice thickness=2.5 mm, phase encoding=PA, nine b0 images (PA), three additional b0 images (AP)).

Fifty-five subjects were scanned in the morning, while the remaining half (56/111) in the afternoon.

2.3 Regions of interest segmentation

T1-weighted images (T1w) were pre-processed and segmented using FreeSurfer 7.11 to obtain binary mask of WM and BG. To reduce the odds of PVS misclassification and partial volume effects, the binary WM mask underwent erosion by one voxel, followed by the subtraction of a dilated mask of the lateral ventricles.

2.3 White matter lesion segmentation

White matter lesions (WML) were segmented applying the lesion growth algorithm (LGA) as implemented in the Lesion Segmentation Tool (LST) toolbox version 3.0.0 (www.statistical-modelling.de/lst.html) from Statistical Parametric Mapping (SPM12, Wellcome Trust Centre for Neuroimaging), setting the initial k value to 0.2. The resulting probability map was then binarized using a threshold of 0.5.

Tissue probability maps of grey matter (GM), WM and CSF generated in the first step of the LGA were also used for total intracranial volume (TIV) calculation. The WML (WMLVF; WMLVF = WML volume/TIV) and GM (GMVF; GMVF = GM volume/TIV) volume fractions were obtained to correct for interindividual brain size variability.

2.4 PVS rating and segmentation

Enlarged PVS were assessed both visually and quantitatively. First, according to Paradise[14] et al., the number of enlarged PVS in the slices located 2 mm (BG_vis) and 37 mm (CSO_vis) above the anterior commissure and their sum (ALL_vis) were counted by LS, a neurologist trained in PVS scoring. PVS were defined according to the Standards for Reporting Vascular Changes on Neuroimaging (STRIVE) criteria[40,41]. PVS of any diameter were included if they fulfilled other STRIVE diagnostic criteria.

Then, PVS were mapped from T1w images using an automated quantification method as follows. Native T1w images were denoised using the non-local mean algorithm available in the scikit-image library 0.21 (https://scikit-image.org/)[42], N4 bias corrected[43] and skull-stripped. Then, Frangi filter[44] was applied to preprocessed T1w images using the scikit-image library 0.21, and setting default parameters with a scale range of 0.5-5 voxels to maximize vessel inclusion. The resulting vesselness map was then binarized using a raw threshold of 0.05 for WM and 0.1 for BG, determined by consensus among LS, FD and CC after visual inspection of the Frangi output. To eliminate PVS mis-segmentation caused by WM hyperintensity, WML were excluded from the PVS mask. The PVS volume fraction (PVSVF; PVSVF = PVS volume/TIV) was measured in the WM and BG and then added to obtain the volume of all PVS (ALL).

2.5 FW and MK calculation

DW images were first corrected for susceptibility induced distortions using the FSL TopUp function (FSL, version 6.0.1) and the additional b0 images, followed by eddy-current correction[45]. To address motion-associated signal dropout, slice-wise outliers were estimated and replaced using Gaussian Process prediction[45].

Maps of the fractional volume of FW and of the MK were constructed from preprocessed DW images fitting a regularized bitensor model and the DKI, respectively, with the open-source software package Diffusion Imaging in Python (Dipy) algorithm (dipy.org/)[46]. A 3D Gaussian smoothing kernel (FWHM=1.25 mm) was applied to the DW images before fitting the model.

Images were then co-registered to their corresponding high resolution T1w image using SPM12.

Mean white matter FW (FW-WM) and MK (MK-WM) values were measured within each WM mask, after excluding WML and PVS and reslicing the WM mask to match the resolution of the DW images, thus including the normal appearing WM only.

2.6 DTI ALPS

The DTI-ALPS index was calculated from DW images using a semi-automated and highly reliable pipeline developed and validated by Taoka et al.[47].

Fractional anisotropy (FA) and mean diffusivity (MD) maps as well as diffusivity maps along the directions of the x-axis (right–left; Dxx), y-axis (anterior–posterior; Dyy), and z-axis (inferior–superior; Dzz) were obtained from preprocessed DW images applying the DTI model with Dipy. The FA maps from all participants were first linearly and then nonlinearly registered to the high-resolution FMRIB58_FA standard space image. The subject with the smallest degree of warping was selected for the regions of interest (ROIs) placement. Using this subject's color-coded FA map, 5 mm spherical ROIs were placed in the projection and

association areas at the level of the lateral ventricle bodies in the left and right hemispheres. ROIs positioning was visually checked in each participant, and manual corrections were performed where needed.

The ALPS index was calculated as reported by Taoka et al.[21]. Left hemisphere ALPS (ALPS_left), right hemisphere ALPS (ALPS_right) and their average (ALPS_mean) were obtained. Average FA and MD of the normal appearing WM were also derived.

2.7 CSF AQP4 and protein determination

Available CSF samples were centrifuged at 1,500×g for 10 min at 4°C. The supernatants were aliquoted in polypropylene tubes and stored at –80◦C until use. CSF levels of Aβ42, total tau (T-tau), and phosphorylated tau at 181 (P-tau) were assessed using either a ChemiLuminescence Enzyme ImmunoAssay (CLEIA) by a Lumipulse G600II platform (Fujirebio, Ghent, Belgium). The following normality thresholds were used: >640 pg/mL for Aβ42, <61 pg/mL for P-tau and <580 pg/mL for T-tau[48].

AQP4 concentration was determined in all available samples of CSF using a specific ELISA kit from Cusabio (www.cusabio.com), as detailed elsewhere[38,37].

Statistical analysis

Data were analyzed using R. 4.3.1. Considering that, except for MK-WM, all variables exhibited significant skewness, non-parametric testing was favoured. The Kruskal-Wallis tests was employed to assess differences in demographic and clinical characteristics among all groups. Generalized linear models were utilized to investigate differences in GS biomarkers, employing a gamma distribution and a log link function, while incrementally entering additional covariates.

In the basic model (Model 1), age, sex, years of formal education and – for MRI indices only – scanning time (dichotomous) were included. Model 2 incorporated WMLVF and Model 3 WMLVF and GMVF as covariates to account for the influence of WM macrostructural damage and GM atrophy. Model 1 was employed to evaluate differences in all biomarkers; Model 2 and 3 were specifically applied when analysing MRI parameters (i.e. all except AQP4). Two runs of analysis were conducted, the first one including all patients; the second one after dividing both patients with AD and patients with other neurodegenerative diseases into two subgroups, based on the degree of GM atrophy using the median value of GMVF in each subgroup. Statistical significance was set at an uncorrected p-value of <0.05.

Finally, partial Spearman rank correlation tests, adjusted for age, sex and years of education were conducted to assess reciprocal associations among putative GS biomarkers and their potential relationships with AD CSF biomarkers and Mini-Mental State Examination (MMSE) scores. The false discovery rate (fdr) was used to correct for multiple correlation tests.

3 Results

3.1 Demographic and clinical characteristics of the study population

A total of 111 subjects were included in the study. Seventy-one of them were diagnosed as suffering from a neurodegenerative disease according to the most recent diagnostic criteria available for each condition[49–54]: forty-seven patients with AD while 11 with FTD, 6 with DLB and 7 with other neurodegenerative disease (non-AD [nAD]=24). Based on their clinical follow-up, 17 subjects were diagnosed with stable MCI while 23 were classified as CU individuals.
Fifty out of 111 participants also underwent lumbar puncture for CSF analysis and 49/50 samples were available for AQP4 measurement (nAD=12, AD=29, MCI=4, CU=4).
Demographic and clinical characteristics of the study population are summarized in Table 1. Notably, MCI patients were less educated than AD patients (p=0.02). No differences in age, sex and disease duration were found between groups.

3.2 Group comparisons in the whole cohort

AQP4 levels were significantly higher in AD (exp(b)=2.05, [Confidence Interval (CI)=1.25-3.21], p=0.005) and nAD patients (exp(b)=2.98, CI=[1.76-4.85], p<0.001) compared to CU individuals. Patients with AD showed a higher FW-WM (exp(b)=1.06, CI=[1.00-1.11], p=0.043) than CU individuals (**Figure 1**).
In Model 2 and 3, AD patients still showed significantly higher FW-WM than CU subjects (exp(b)=1.06, CI=[1.01-1.12], p=0.028 in Model 2; exp(b)=1.06, CI=[1.01-1.12], p=0.031 in Model 3)(**Figure 4A**).

3.3 Group comparisons including only degenerative patients with less GM atrophy

When considering AD (n=23) and nAD (=12) patients with less GM atrophy, AQP4 and FW-WM were significantly higher in the AD (exp(b)=2.20, CI=[1.29-3.59], p=0.006; exp(b)=1.08, CI=[1.01-1.15], p=0.019, respectively) and in the nAD groups (exp(b)=2.66, CI=[1.50-4.62], p=0.002; exp(b)=1.10, CI=[1.02-1.19], p=0.019, respectively) compared to CU subjects (**Figure 2**). In Models 2 and 3, FW-WM was still higher in both AD (exp(b)=1.08, CI=[1.01-1.15], p=0.023, Model 2; exp(b)=1.08, CI=[1.01-1.15, p=0.029, Model 3) and nAD groups (exp(b)=1.10, CI=[1.02-1.19], p=0.021, Model 2; exp(b)=1.10, CI=[1.02-1.19], p=0.023, Model 3) compared to CU individuals (**Figure 4B**).

3.4 Group comparisons including only degenerative patients with higher GM atrophy

When focusing on AD (n=24) and nAD (n=12) patients with more remarkable GM atrophy, the former group showed higher CSO_vis (exp(b)=1.89, CI=[1.15-3.10], p=0.016), ALL_vis (exp(b)=1.59, CI=[1.12-2.24], p=0.013), PVSVF_WM (exp(b)=1.89, CI=[1.23-2.90], p=0.005) and PVSVF_ALL (exp(b)=1.50, CI=[1.04-2.16], p=0.036) together with lower MK-WM (exp(b)=0.94, CI=[0.90-0.98], p=0.006), ALPS_mean (exp(b)=0.91, CI=[0.84-0.99], p=0.043) and ALPS_left (exp(b)=0.88, CI=[0.81-0.97], p=0.010). Moreover, nAD patients showed higher levels of AQP4 (exp(b)=3.39, CI=[1.76-6.49], p=0.002) compared to CU individuals, while, in the same comparison, AD patients showed a trend towards statistical significance only (p=0.052) (**Figure 3**).

In Model 2, CSO_vis (exp(b)=2.42, CI=[1.47-3.97], p<0.001), ALL_vis (exp(b)=1.72, CI=[1.21-2.46], p=0.005) and PVSVF_WM (exp(b)=1.64, CI=[1.08-2.48], p=0.025) remained significantly higher, whereas ALPS_left significantly lower (exp(b)=0.90, CI=[0.82-0.99], p=0.036) in AD patients compared to CU subjects. Conversely, differences in MK-WM, PVSVF_ALL and ALPS_mean did no longer reach statistical significance.

In Model 3, results obtained in Model 2 were partially preserved. AD patients still showed higher CSO_vis (exp(b)=2.54, CI=[1.39-4.58], p=0.002), ALL_vis (exp(b)=1.83, CI=[1.19-2.79], p=0.006), PVSVF_WM (exp(b)=2.07, CI=[1.27-3.32], p=0.004) and PVSVF_ALL (exp(b)=1.59, CI[1.05-2.41], p=0.029) than CU. However, the observed difference in ALPS_left was no longer significant (**Figure 4C**).

3.5 Correlation analysis in the whole population

Considering the entire study population, CSO_vis exhibited positive association with increased FW-WM (p_{fdr}<0.001). MK-WM was positively correlated with ALPS_right and ALPS_mean (rho=0.29, p_{fdr}=0.019; rho=0.27, p_{fdr}=0.046 respectively). GS MRI parameters were not associated with CSF biomarkers of AD nor MMSE in the whole population.

3.6 Correlation analysis in the AD subgroup

When focusing on patients with AD, higher PVSVF_WM, PVSVF_ALL and CSO_vis were associated with higher FW-WM (rho=0.46, p_{fdr}=0.018; rho=0.44, p_{fdr}=0.028; rho=0.52, p_{fdr}=0.006 respectively). PVSVF_WM and PVSVF_ALL showed a significant negative correlation with ALPS_right (rho=-0.48, p_{fdr}=0.015; rho=-0.37, p_{fdr}=0.027 respectively).

After correction for multiple correlations, lower ALPS_right, ALPS_left and ALPS_mean showed a trend toward association with lower Aβ42 levels (rho=0.57, p_{fdr}=0.095; rho=0.52, p_{fdr}=0.095; rho=0.53, p_{fdr}=0.095 respectively). GS MRI parameters were not associated with MMSE in the AD subgroup.

Uncorrected correlation between GS biomarkers and FA, MD, WMLVF, GMVF, and age are reported in **Supplementary table 1**.

4 Discussion

In this study, we combined the use of non-invasive MRI metrics and measurement of CSF-AQP4 levels to attempt a comprehensive characterization of the GS function in patients suffering from neurodegenerative dementia, with a specific focus on AD.
According to our a priori hypothesis, we observed significant alterations of all the examined biomarkers in patients with AD and, to a lesser extent, in those with other forms of degenerative dementia when compared to CU individuals. In particular, patients with degenerative diseases exhibited higher CSF-AQP4 levels and increased FW-WM compared to CU subjects. Moreover, AD patients compared to CU subjects showed a greater burden of enlarged PVS in the WM, reduced MK and diffusivity along perivascular spaces obtained by ALPS index, though these latter findings were statistically significant only when focusing the analysis on AD patients with higher GM atrophy.
Overall, these findings suggest an alteration of the GS in association with neurodegeneration and AD pathology. However, variations among different patient subgroups and the absence of correlation with cognitive scores require further discussion.

Previous investigations have consistently demonstrated an association between worsening AD pathology and over-expression and loss of perivascular localization of AQP4[33,34]. In line with this, ourselves and other groups have previously described higher levels of AQP4 in the CSF of patients with AD and other forms of degenerative dementia, when compared to healthy controls[37]. Here, we replicated the same finding in an entirely new cohort of patients, which indicates robustness of this observation and its potential pathophysiological value. However, AQP4 levels were not correlated with tau, contrary to previous observations from our group[38,37], and were unrelated to the other biomarkers of glymphatic activity, hindering speculation regarding the pathophysiological origin of AQP4 over-expression.
Further investigation would help to elucidate whether AQP4 may be considered either a proxy measure of glymphatic dysfunction or rather a marker of reactive astrocytosis in the context of neurodegeneration.

The significantly higher FW in the normal appearing WM of patients affected by AD and other neurodegenerative diseases is consistent with previous data[19,24–26]. Indeed, two studies analyzing ADNI data[24,25], along with a third monocentric study from Singapore[26], consistently reported higher FW in the normal appearing WM of AD patients compared to controls. Conversely, we did not observe a significant difference in FW-WM between MCI patients and CU subjects, aligning with findings by Kamagata et al.[24] , but contrasting with those by Dumont

et al.[25]. In our study, increase of FW content was particularly pronounced within the subgroup of neurodegenerative patients exhibiting a lower degree of GM atrophy. Moreover, it was only marginally affected when accounting for WMLVF, in contrast to what has been observed by Kamagata et al.[24], and GMVF.

Taken altogether, these observations indicate that FW might reflect early interstitial water accumulation, which is at least partially independent from WM damage and GM atrophy. This phenomenon might therefore signify expansion and stasis of ISF[55], possibly due to glymphatic dysfunction. However, several non-mutually exclusive mechanisms, including edema, modulation of BBB permeability, and neuroinflammation[56] are known to occur and may result in an increase in extracellular water fraction. The observed association between increase FW-WM and a higher burden of enlarged PVS in the WM may support an interpretation of this metric as a marker of impaired interstitial bulk flow.

Differences in the other biomarkers were only detected in AD patients with a higher degree of GM atrophy compared to CU individuals. This result may prompt some general considerations. First, regarding brain atrophy as a surrogate of disease severity, AQP4 and FW might capture early alterations in glymphatic function, possibly linked to an astrocytic response to damage[57,58]. In contrast, the remaining biomarkers might reflect later pathophysiological aspects of glymphatic decompensation. This for example, has been suggested for ALPS-index[59]. Second, although glymphatic failure is thought to be a common mechanism in neurodegenerative diseases, the distinctive pattern of alterations that we observed in the AD subgroup may imply a specific pathophysiological role of GS dysfunction in AD brains. This is particularly evident in the case of ALPS index and PVS, whose deviations from normal levels were more pronounced in AD patients compared to those with other neurodegenerative dementias. Additional considerations pertaining to individual biomarkers are discussed in the following sections.

When comparing patients with AD and more pronounced GM atrophy against CU subjects, the former showed PVS enlargements more significantly distributed in the WM but not in the BG. Post-mortem studies have reported direct correlations between PVS in the WM, cortical Aβ deposition, CAA severity, and APOE ε4 polymorphism[10,60,61]. Nonetheless, some studies failed to identify an association between PVS in the WM and amyloid load, as assessed by either positron emission tomography[62,63] or CSF-Aβ levels[27,93]. A possible explanation for this inconsistency is that enlarged PVS in the WM are associated with AD but not Aβ biomarkers because they are manifestations amyloid-independent processes of AD, for example a tau protein-related process. In fact, ourselves and other groups have previously described a significant association between tau levels in the CSF[55,27] or tau deposition[62] and enlarged

PVS, particularly in the CSO[64]. Indeed, differences in PVS burden in the WM of AD patients were enhanced by the inclusion of WMLVF and GMVF as confounding factors. This suggests that enlarged PVS burden in AD exceeds what is associated with vascular pathology and could be linked to accelerated neurodegeneration secondary to GS dysfunction.

DKI derived metrics were recently identified as a potential biomarker of glymphatic clearance[31]. According to available data, we hypothesized a reduction in MK of the normal appearing WM associated with ISF expansion secondary to GS dysfunction. We observed the expected changes when comparing patients with higher levels of atrophy against CU individuals. This was not the case when comparing the whole cohort of patients or the less atrophic subgroup to CU subjects. Considering GM atrophy as a proxy of disease stage, these findings may be partially explained by the nonlinear relationship between amyloid burden and changes in WM diffusivity[65,66] across disease progression. We argue that the less remarkable changes in WM diffusivity seen at early AD stages may reflect a mixture of compensating and inflammatory mechanisms, which are followed by more widespread changes in diffusivity driven by neurodegeneration. Moreover, MK values were strongly dependent on GMVF, aging and measures of WM integrity (**Supplementary table 1**). This suggests that MK reduction may primarily reflect myelin sheath damage and decreased axonal density. In contrast to other techniques (e.g. FW), MK is likely unable to single out the increase in interstitial volume fraction due to GS dysfunction and ISF stasis in the context of neurodegeneration.

Overall, previous studies reported a significant decrease in ALPS index of AD patients, and less consistently MCI[67,68], as compared to controls[69,67,24,68,21]. Our findings are partially consistent with these data. We observed a significant reduction of ALPS index in AD patients with more GM atrophy, but not in the less atrophic subgroup. Moreover, we did not detect any significant difference between patients with MCI and CU, in contrast to results by Steward et al.[68] and Zhong et al.[67] but as already described by Kamagata et al.[24]. The inconsistent findings in relation to MCI patients may be due to the lack of consensus about the clinical diagnostic criteria and their operationalization in different studies, leading to prominent heterogeneity of the MCI groups across different studies. Indeed, a recent study by Huang et al.[70] found significantly lower ALPS index values in amyloid-positive, but not amyloid negative MCI patients compared to controls. Considering the defining features of our MCI group, this result may help explain our finding. Conversely, the absence of significant differences in ALPS-indices when incorporating less atrophic patients needs to be further addressed. Most of our AD patients could be classified as mild. By contrast, previous studies have mostly included AD patients at more advanced disease stages[67,69,68,21], which could partially account for some of the inconsistencies. Interestingly, in a recent study by Kamagata et al. a significant

reduction of mean ALPS index was detectable even in patients with rather mild AD who were selected from the ADNI database. Given the comparable sample size and the similar statistics, such a discrepancy might be attributable to their incorporation of APOE ε4 as a confounding factor. Unfortunately, we do not have APOE ε4 data available for our cohort of patients to further support this speculation.

Moreover, as already pointed out by Kamagata et al., the differences in ALPS indices were significantly reduced after the inclusion of WMLVF as covariate, and disappeared after the additional incorporation of GMVF in the models, indicating the influence of WML and GM atrophy on measures of glymphatic dysfunction in AD brains[71–75]. However, based on their own findings, Hsu et al. have recently proposed that the decline in the ALPS index may precede and partially mediate GMVF alterations in individuals with AD[71]. Furthermore, Huang et al. observed that the abnormality of ALPS index prominently increased before the threshold of CSF Aβ42 positivity and then plateaued[70]. Nevertheless, in the absence of any conclusive evidence from longitudinal data or animal models[76,77,3], an alternative interpretation is that changes in ALPS index might represent a late epiphenomenon of structural brain damage.

The strong association between ALPS index, WM damage and GM atrophy may also explain its association with patient cognitive scores, particularly with the MMSE of more atrophic patients[69,67,71,21]. We did not detect any association in the whole cohort. This is contrary to findings in most prior studies but aligns with recent research by Matsushita et al.[78]. In both cases, disagreement may be attributable to patient stratification (predominantly very mild to mild AD) and the relatively narrow range of MMSE scores.

As previously described[24], we also observed a trend toward association between ALPS index in the left hemisphere and CSF-Aβ42 in the AD subgroup. It is notable that the observed trend was specific to the left ALPS. This could be attributed to anatomical differences between the two hemispheres and the inclusion of patients affected by progressive aphasia, which primarily impacts the left hemisphere. Nonetheless, the relationship between ALPS index and amyloid deposition in the cerebral cortex remains unclear[71,78] and requires further investigations.

In summary, according to our study, ALPS index may behave like a proxy measure of late GS failure associated with neurodegeneration, rather than an early biomarker of glymphatic dysfunction. On the other hand, the distinct changes observed in ALPS within the AD subgroup and its correlation with Aβ suggest a specific association with accumulation of AD pathology.

5 Limitations

The major limitation of this study is the lack of direct pathophysiological support to our measures. At the time of writing, only the DTI-ALPS index had been directly correlated with measures obtained with GBCA CSF tracers[5]. However, concerns still remain about its true

capacity to represent glymphatic clearance, primarily based on anatomical considerations[79]. Since the exact histopathologic processes underlying the observed alterations is not fully understood, our results need to be interpreted with caution.

Second, we only evaluated cross-sectional data from a single memory clinic. Future studies should focus on the longitudinal changes of these biomarkers and their interactions with amyloid and tau protein deposition and measure of cognitive dysfunction.

Third, the subgroups of MCI and CU individuals with available AQP4 dosing were rather small, because we prioritized homogeneity of the sample. However, statistical significances did not change when 1) joining MCI and CU groups AND 2) adding all CU patients with available AQP4 measurements from our lab (8 additional subjects) (**Supplementary figure 1**).

Fourth, our PVS segmentation relied solely on T1w images due to the unavailability of T2 volumetric scans, in contrast to what has been suggested by Sepehrband et al. to enhance PVS contrast[17]. We also acknowledge the limitations of the PVS segmentation method. To deal with this limitation and strengthen our findings, we associated visual rating scores to volumetric PVS quantification.

Another limitation is that AQP4 genetic and APOE ε4 allelic variations were not included as confounding factors due to unavailability. AQP4 mutations are known to modulate glymphatic activity and associate with Aβ clearance[80,81], while APOE allelic mutations may impact the number of PVS[13,82]. Furthermore, despite the exclusion of subjects with significant vascular brain damage, we did not control for cardiovascular risk factors and sleep disturbances, which are both known to influence glymphatic activity.

Lastly, we used GM atrophy to identify patients at different stages of the disease. Though evidence for this choice is sound[83–85], cognitive scores or severity scale could have been used instead. However, CDR was not available for all the participants, while the MMSE sensitivity is lower in the early stages of the disease due to cognitive reserve[86,87] and ceiling effect[88,89]. Moreover, it could not be representative of the disease stage in patients affected by subtypes of progressive aphasia, who were present, though rare, in both the nAD and the AD groups in our study.

6 Conclusions

Our results revealed that AQP4 and FW-WM are significantly increased in patients with neurodegenerative dementia compared to CU subjects at the early stages of the disease as assessed by lower levels of GM atrophy. Additionally, we confirmed substantial GS alterations in more advanced AD patients, characterized by an increased burden of enlarged PVS in the WM, lower MK and lower DTI-ALPS. DTI-ALPS may also serve as a marker of disease progression in AD.

While the bulk of these findings align with existing literature reporting significant alterations of putative GS biomarkers in neurodegenerative diseases, particularly AD, we hereby describe a heavy dependency of some of these indices, particularly MK-WM and DTI-ALPS, on measures of structural brain damage. This may partly hinder their usefulness as standalone and indirect markers of glymphatic activity until validated by comparative studies against established gold standard.

Notwithstanding this limitation, our results suggest a close interaction between glymphatic function and neurodegeneration, particularly in the case of AD. This interaction could potentially serve as a target for dementia prevention, by managing physiological factors like sleep hygiene[90] and cardiovascular risk[91], which are known to influence GS activity. In addition, in patients who are already suffering from cognitive decline, this might represent a potential target for therapeutic interventions, whether pharmacological[92] or physical[93], capable of modulating glymphatic clearance.

Table 1. Demographics and clinical characteristics of the study population

	nAD	AD	MCI	CU	*p* value (fdr)						
	n=24	n=47	n=17	n=23	nADvsADvsMCIvsCU	nADvs AD	nADvs MCI	ADvs MCI	nADvs CU	Advs CU	MCIvs CU
Sex (M/F)	9/15	22/25	8/9	14/9	0.36						
Age (y)	75 (70.75, 77.25)	71 (67.5,76)	74 (69,76)	70 (60, 75.5)	0.12						
Education (y)	13 (7.75, 14.25)	13 (12,18)	8 (8,13)	13 (8, 18)	**0.042**			**0.031**			
Disease duration (y)	3.02 (2.32, 5.6)	2.51 (1.69, 4.69)	2.73 (1.70, 3.48)	2.80 (2.30, 4.22)	0.49						
MMSE (N)	24 (18.75, 26)	23 (20.5,26)	27 (25, 28)	29 (28, 30)	**<0.001**		**0.012**	**0.001**	**<0.001**	**<0.001**	**0.001**
Aβ42 (pg/mL)	829 (700, 891)	496 (435, 591)	1218 (1158.5, 1330)	854 (762, 945)	**<0.001**	**<0.001**	**0.038**	**0.001**		**0.002**	
T-tau (pg/mL)	518 (192, 851)	669 (407, 922)	252 (205, 261)	501 (276, 750)	0.056						
P-tau (pg/mL)	84 (33, 119)	122 (68, 154)	34 (30, 35)	88 (34, 140)	**0.049**						
T-tau/Aβ42	0.78 (0.24, 1.11)	1.29 (0.78, 1.93)	0.19 (0.16, 0.21)	0.53 (0.38, 0.75)	**<0.001**	**0.017**	**0.038**	**0.002**		**0.031**	
P-tau/Aβ42	0.12 (0.03, 0.17)	0.22 (0.15, 0.32)	0.02 (0.02, 0.03)	0.09 (0.05, 0.14)	**<0.001**	**0.007**	**0.046**	**0.002**		**0.046**	
WMLVF	0.004 (0.002, 0.008)	0.003 (0.002, 0.007)	0.003 (0.001, 0.008)	0.002 (0.0006, 0.004)	0.1						
GMVF	0.371 (0.344, 0.425)	0.387 (0.354, 0.425)	0.418 (0.379, 0.454)	0.421 (0.398, 0.457)	**0.013**		**0.03**	**0.03**			

Abbreviations: Aβ42 = amyloid β 42; AD = Alzheimer's disease patients; CU = cognitively unimpaired subjects; GMVF = gray matter volume fraction; MCI = mild cognitive impairment patients; MMSE = Mini-Mental State Examination; nAD = non Alzheimer's disease degenerative patients; P-tau = phosphorylated tau; T-tau = total tau; WMLVF = white matter lesion volume fraction;

Data are presented as median (Q1,Q3). N represents the number of patients. *p* values reported in bold denote statistical significance at $p < 0.05$ (Kruskal-Wallis test, FDR corrected).

Figures

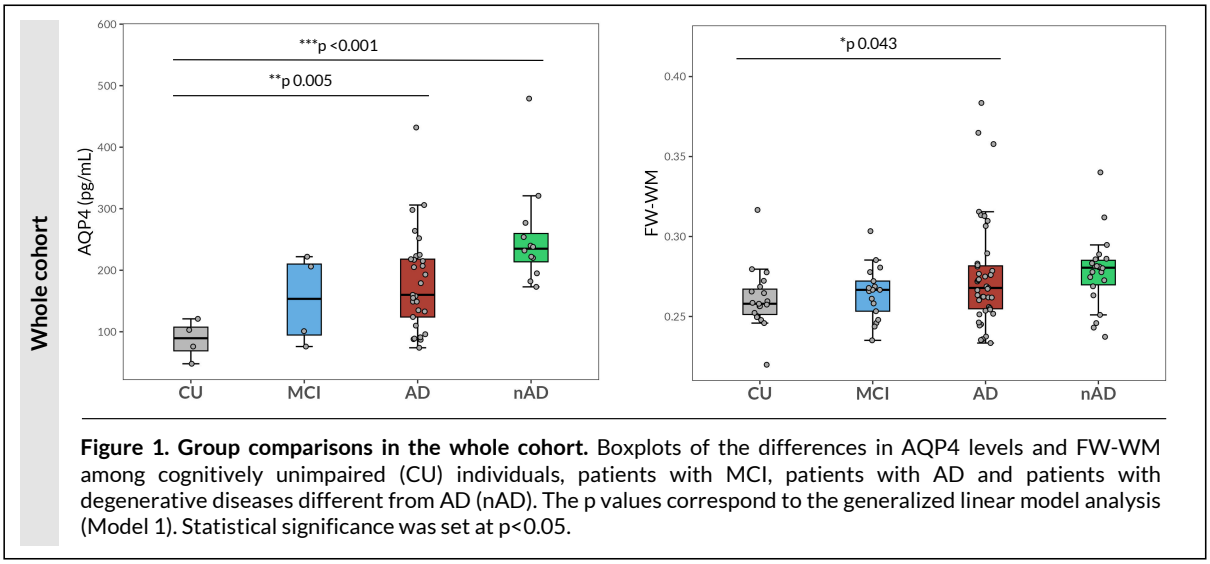

Figure 1. Group comparisons in the whole cohort. Boxplots of the differences in AQP4 levels and FW-WM among cognitively unimpaired (CU) individuals, patients with MCI, patients with AD and patients with degenerative diseases different from AD (nAD). The p values correspond to the generalized linear model analysis (Model 1). Statistical significance was set at p<0.05.

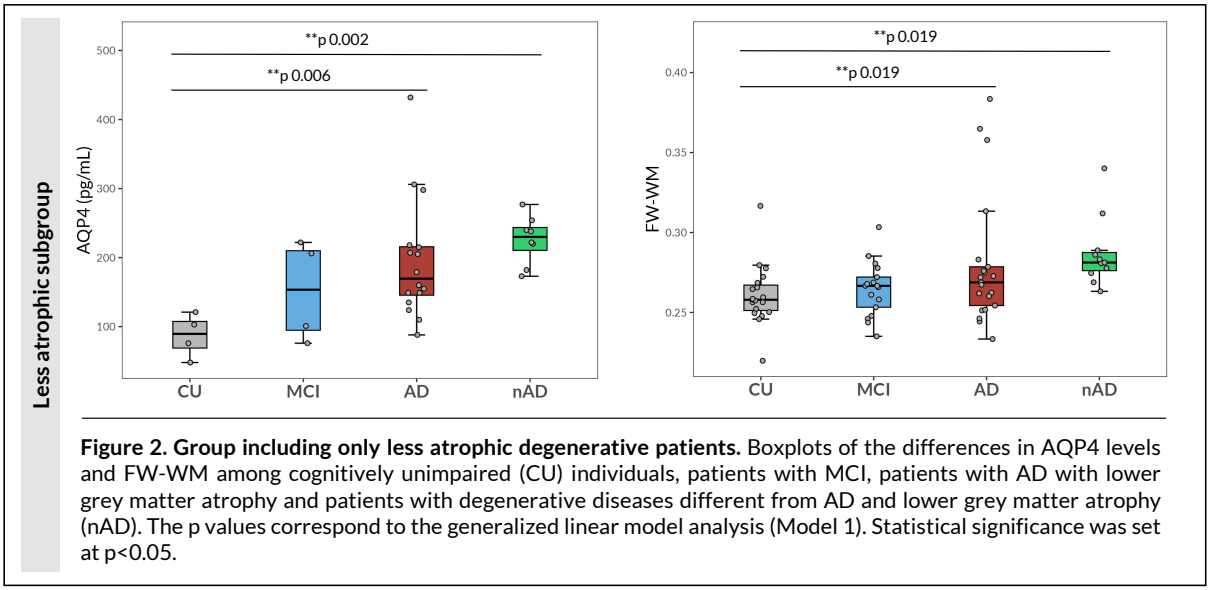

Figure 2. Group including only less atrophic degenerative patients. Boxplots of the differences in AQP4 levels and FW-WM among cognitively unimpaired (CU) individuals, patients with MCI, patients with AD with lower grey matter atrophy and patients with degenerative diseases different from AD and lower grey matter atrophy (nAD). The p values correspond to the generalized linear model analysis (Model 1). Statistical significance was set at p<0.05.

Figure 2. Group including only less atrophic degenerative patients. Boxplots of the differences in AQP4 levels and FW-WM among cognitively unimpaired (CU) individuals, patients with MCI, patients with AD with lower grey matter atrophy and patients with degenerative diseases different from AD and lower grey matter atrophy (nAD). The p values correspond to the generalized linear model analysis (Model 1). Statistical significance was set at p<0.05.

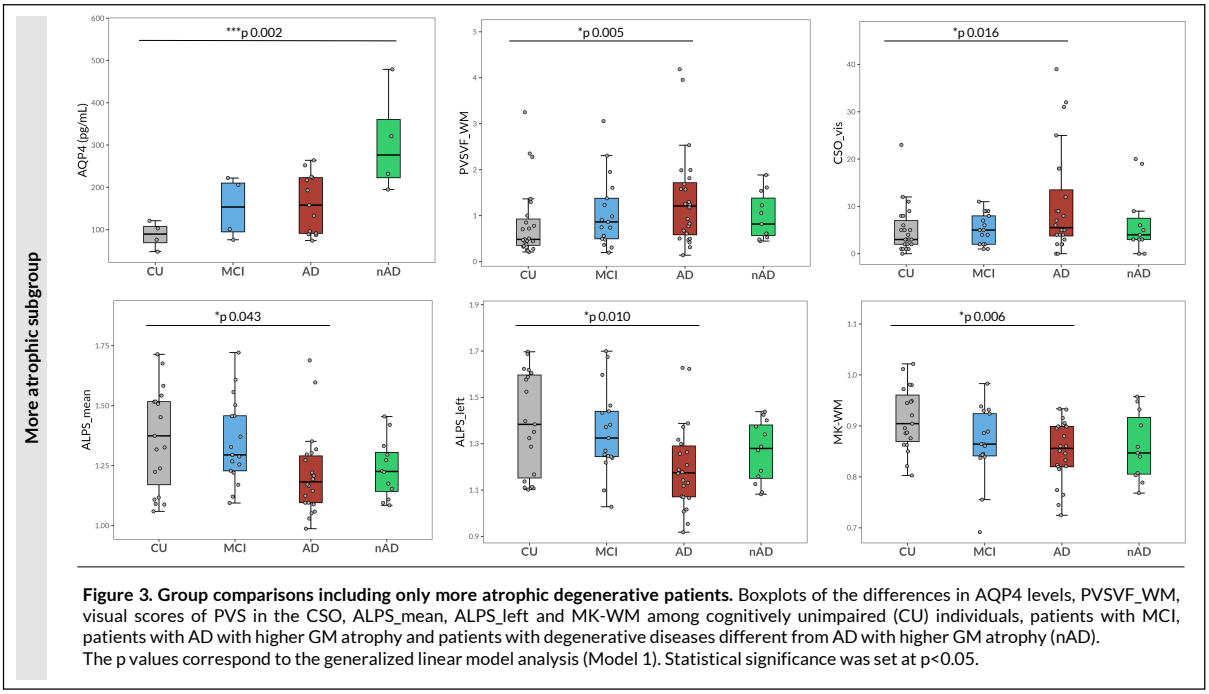

Figure 3. Group comparisons including only more atrophic degenerative patients. Boxplots of the differences in AQP4 levels, PVSVF_WM, visual scores of PVS in the CSO, ALPS_mean, ALPS_left and MK-WM among cognitively unimpaired (CU) individuals, patients with MCI, patients with AD with higher GM atrophy and patients with degenerative diseases different from AD with higher GM atrophy (nAD).
The p values correspond to the generalized linear model analysis (Model 1). Statistical significance was set at p<0.05.

Figure 3. Group comparisons including only more atrophic degenerative patients. Boxplots of the differences in AQP4 levels, PVSVF_WM, visual scores of PVS in the CSO, ALPS_mean, ALPS_left and MK-WM among cognitively unimpaired (CU) individuals, patients with MCI, patients with AD with higher GM atrophy and patients with degenerative diseases different from AD with higher GM atrophy (nAD).

The p values correspond to the generalized linear model analysis (Model 1). Statistical significance was set at p<0.05.

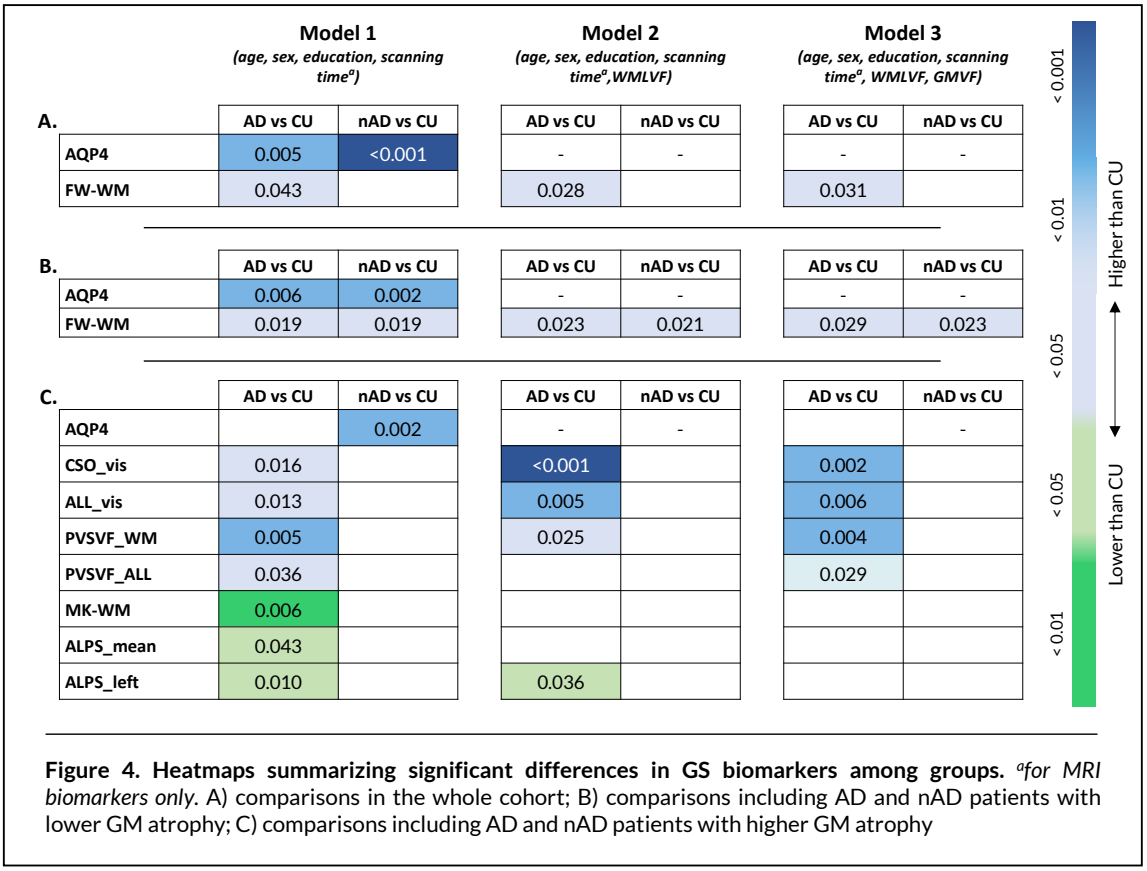

Figure 4. Heatmaps summarizing significant differences in GS biomarkers among groups. *[a]for MRI biomarkers only.* A) comparisons in the whole cohort; B) comparisons including AD and nAD patients with lower GM atrophy; C) comparisons including AD and nAD patients with higher GM atrophy

Figure 4. Heatmaps summarizing significant differences in GS biomarkers among groups. [a]*for MRI biomarkers only*. A) comparisons in the whole cohort; B) comparisons including AD and nAD patients with lower GM atrophy; C) comparisons including AD and nAD patients with higher GM atrophy

Supplementary material

Supplementary table 1. Correlation analysis between biomarkers of glymphatic function, age and measures of white matter and grey matter damage

a. Whole cohort

	FA		MD		WMLVF		GMVF		Age	
	rho	*p* value	rho	*p* value	rho	*p* value	rho	*p* value	rho	*p* value
AQP4										
CSO_vis										
BG_vis	-0.24	0.018			0.28	0.004			0.21	0.031
ALL_vis										
PVSVF_WM	-0.31	0.002			0.53	<0.001				
PVSVF_BG			-0.29	0.004						
PVSVF_ALL	-0.30	0.003			0.49	<0.001				
FW-WM	-0.30	0.002	0.72	<0.001						
MK-WM	-0.90	<0.001	-0.49	<0.001	-0.68	<0.001	0.43	<0.001	-0.35	<0.001
ALPS_mean					-0.40	<0.001	0.37	<0.001	-0.35	<0.001
ALPS_left					-0.39	<0.001	0.32	0.001	-0.35	<0.001
ALPS_right					-0.40	<0.001	0.38	<0.001	-0.32	<0.001

b. Alzheimer's disease subgroup

	FA		MD		WMLVF		GMVF		Age	
	rho	*p* value	rho	*p* value	rho	*p* value	rho	*p* value	rho	*p* value
AQP4										
CSO_vis			0.34	0.027						
BG_vis										
ALL_vis										
PVSVF_WM	-0.41	0.006			0.58	<0.001	-0.32	0.031		
PVSVF_BG			-0.41	0.007						
PVSVF_ALL	-0.38	0.013			0.58	<0.001				
FW-WM	-0.37	0.014	0.71	<0.001						
MK-WM	-0.91	<0.001	-0.51	<0.001	-0.66	<0.001	0.36	0.014	-0.44	0.003
ALPS_mean					-0.54	<0.001	0.53	<0.001	-0.36	0.015
ALPS_left					-0.50	<0.001	0.50	<0.001	-0.36	0.016
ALPS_right	0.32	0.045			-0.57	<0.001	0.53	<0.001	-0.36	0.017

Abbreviations: ALL_vis = all perivascular spaces, visual score; ALPS = DTI analysis along the perivascular spaces; AQP4 = aquaporin-4; BG_vis = basal ganglia perivascular spaces, visual score; CSO_vis = centrum semiovale perivascular spaces, visual score ; FA = avarage fractional anisotropy of the normal appearing white matter; FW-WM = average value of free water value of the normal appearing white matter; MD = avarage mean diffusivity of the normal appearing white matter; MK-WM = average value of the mean kurtosis of the normal appearing white matter; GMVF = gray matter volume fraction; PVSVF = perivascular spaces volume fraction; WMLVF = white matter lesion volume fraction; .
Results of uncorrected Spearman's correlation test. Reported *p* values denote statistical significance at p<0.05

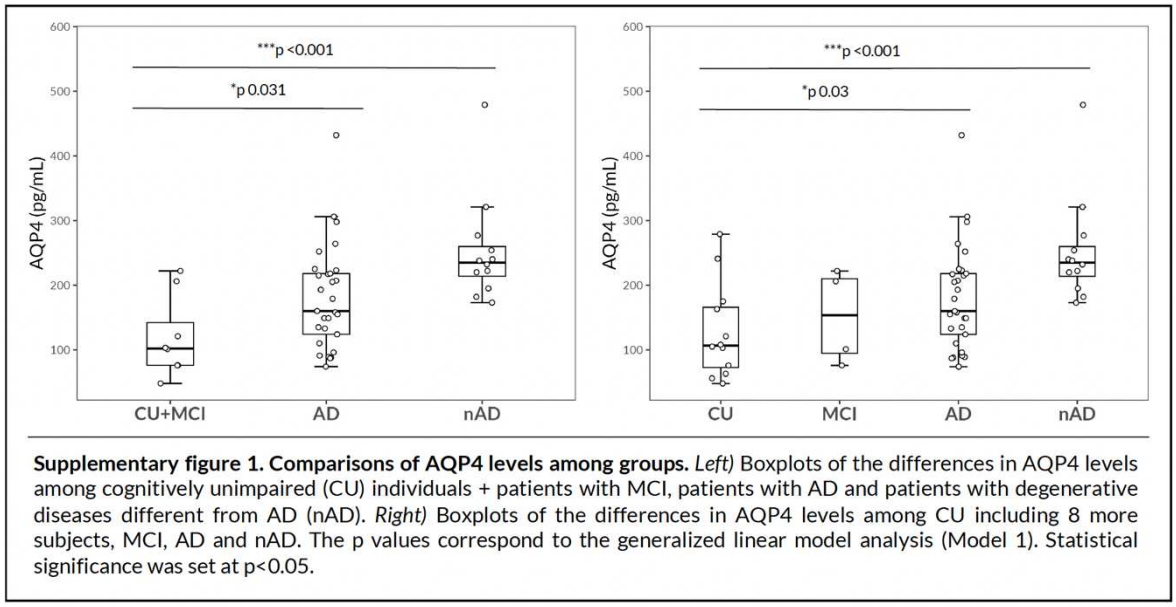

Supplementary figure 1. Comparisons of AQP4 levels among groups. *Left)* Boxplots of the differences in AQP4 levels among cognitively unimpaired (CU) individuals + patients with MCI, patients with AD and patients with degenerative diseases different from AD (nAD). *Right)* Boxplots of the differences in AQP4 levels among CU including 8 more subjects, MCI, AD and nAD. The p values correspond to the generalized linear model analysis (Model 1). Statistical significance was set at p<0.05.

Supplementary figure 1. Comparisons of AQP4 levels among groups. Left) Boxplots of the differences in AQP4 levels among cognitively unimpaired (CU) individuals + patients with MCI, patients with AD and patients with degenerative diseases different from AD (nAD). Right) Boxplots of the differences in AQP4 levels among CU including 8 more subjects, MCI, AD and nAD. The p values correspond to the generalized linear model analysis (Model 1). Statistical significance was set at p<0.05.

References

1. Bohr, T. *et al.* The glymphatic system: Current understanding and modeling. *iScience* **25**, 104987 (2022).
2. Rasmussen, M. K., Mestre, H. & Nedergaard, M. The glymphatic pathway in neurological disorders. *The Lancet Neurology* **17**, 1016–1024 (2018).
3. Iliff, J. J. *et al.* A Paravascular Pathway Facilitates CSF Flow Through the Brain Parenchyma and the Clearance of Interstitial Solutes, Including Amyloid β. *Sci. Transl. Med.* **4**, (2012).
4. Zhou, Y. *et al.* Impairment of the Glymphatic Pathway and Putative Meningeal Lymphatic Vessels in the Aging Human. *Annals of Neurology* **87**, 357–369 (2020).
5. Zhang, W. *et al.* Glymphatic clearance function in patients with cerebral small vessel disease. *NeuroImage* **238**, 118257 (2021).
6. Zhang, M. *et al.* Evaluation of glymphatic-meningeal lymphatic system with intravenous gadolinium-based contrast-enhancement in cerebral small-vessel disease. *Eur Radiol* **33**, 6096–6106 (2023).
7. Schubert, J. J. *et al.* Dynamic ^{11} C-PiB PET Shows Cerebrospinal Fluid Flow Alterations in Alzheimer Disease and Multiple Sclerosis. *J Nucl Med* **60**, 1452–1460 (2019).
8. Evans, T. E. *et al.* Determinants of Perivascular Spaces in the General Population: A Pooled Cohort Analysis of Individual Participant Data. *Neurology* **100**, e107–e122 (2023).
9. Bown, C. W., Carare, R. O., Schrag, M. S. & Jefferson, A. L. Physiology and Clinical Relevance of Enlarged Perivascular Spaces in the Aging Brain. *Neurology* **98**, 107–117 (2022).
10. Perosa, V. *et al.* Perivascular space dilation is associated with vascular amyloid-β accumulation in the overlying cortex. *Acta Neuropathol* **143**, 331–348 (2022).
11. Kim, H. J. *et al.* MRI-Visible Perivascular Spaces in the Centrum Semiovale Are Associated with Brain Amyloid Deposition in Patients with Alzheimer Disease–Related Cognitive Impairment. *AJNR Am J Neuroradiol* **42**, 1231–1238 (2021).
12. Charidimou, A. *et al.* White matter perivascular spaces: An MRI marker in pathology-proven cerebral amyloid angiopathy? *Neurology* **82**, 57–62 (2014).
13. Paradise, M. *et al.* Association of Dilated Perivascular Spaces With Cognitive Decline and Incident Dementia. *Neurology* **96**, e1501–e1511 (2021).
14. Paradise, M. B. *et al.* Development and validation of a rating scale for perivascular spaces on 3T MRI. *Journal of the Neurological Sciences* **409**, 116621 (2020).
15. Pham, W. *et al.* A critical guide to the automated quantification of perivascular spaces in magnetic resonance imaging. *Front. Neurosci.* **16**, 1021311 (2022).
16. Barisano, G. *et al.* Imaging perivascular space structure and function using brain MRI. *Neuroimage* **257**, 119329 (2022).
17. Sepehrband, F. *et al.* Image processing approaches to enhance perivascular space visibility and quantification using MRI. *Sci Rep* **9**, 12351 (2019).
18. Ballerini, L. *et al.* Perivascular Spaces Segmentation in Brain MRI Using Optimal 3D Filtering. *Sci Rep* **8**, 2132 (2018).
19. Bergamino, M., Walsh, R. R. & Stokes, A. M. Free-water diffusion tensor imaging improves the accuracy and sensitivity of white matter analysis in Alzheimer's disease. *Sci Rep* **11**, 6990 (2021).
20. Pierpaoli, C., Jezzard, P., Basser, P. J., Barnett, A. & Di Chiro, G. Diffusion tensor MR imaging of the human brain. *Radiology* **201**, 637–648 (1996).
21. Taoka, T. *et al.* Evaluation of glymphatic system activity with the diffusion MR technique: diffusion tensor image analysis along the perivascular space (DTI-ALPS) in Alzheimer's disease cases. *Jpn J Radiol* **35**, 172–178 (2017).
22. Jones, D. K. & Cercignani, M. Twenty-five pitfalls in the analysis of diffusion MRI data. *NMR in Biomedicine* **23**, 803–820 (2010).
23. Pasternak, O., Sochen, N., Gur, Y., Intrator, N. & Assaf, Y. Free water elimination and mapping from diffusion MRI. *Magnetic Resonance in Med* **62**, 717–730 (2009).
24. Kamagata, K. *et al.* Association of MRI Indices of Glymphatic System With Amyloid Deposition and Cognition in Mild Cognitive Impairment and Alzheimer Disease. *Neurology* **99**, e2648–e2660 (2022).
25. Dumont, M. *et al.* Free Water in White Matter Differentiates MCI and AD From Control Subjects. *Front. Aging Neurosci.* **11**, 270 (2019).
26. Ji, F. *et al.* Distinct white matter microstructural abnormalities and extracellular water increases relate to cognitive impairment in Alzheimer's disease with and without cerebrovascular disease. *Alz Res Therapy* **9**, 63 (2017).
27. Maier-Hein, K. H. *et al.* Widespread white matter degeneration preceding the onset of dementia. *Alzheimer's & Dementia* **11**, 485 (2015).
28. Maillard, P. *et al.* Cerebral white matter free water: A sensitive biomarker of cognition and function. *Neurology* **92**, e2221–e2231 (2019).

29. Jensen, J. H. & Helpern, J. A. MRI quantification of non-Gaussian water diffusion by kurtosis analysis. *NMR in Biomedicine* **23**, 698–710 (2010).

30. Jensen, J. H., Helpern, J. A., Ramani, A., Lu, H. & Kaczynski, K. Diffusional kurtosis imaging: The quantification of non-gaussian water diffusion by means of magnetic resonance imaging. *Magnetic Resonance in Med* **53**, 1432–1440 (2005).

31. Örzsik, B. *et al.* Higher order diffusion imaging as a putative index of human sleep-related microstructural changes and glymphatic clearance. *NeuroImage* **274**, 120124 (2023).

32. Bergström, S. *et al.* Multi-cohort profiling reveals elevated CSF levels of brain-enriched proteins in Alzheimer's disease. *Ann Clin Transl Neurol* **8**, 1456–1470 (2021).

33. Boespflug, E. L. *et al.* Targeted Assessment of Enlargement of the Perivascular Space in Alzheimer's Disease and Vascular Dementia Subtypes Implicates Astroglial Involvement Specific to Alzheimer's Disease. *JAD* **66**, 1587–1597 (2018).

34. Zeppenfeld, D. M. *et al.* Association of Perivascular Localization of Aquaporin-4 With Cognition and Alzheimer Disease in Aging Brains. *JAMA Neurol* **74**, 91 (2017).

35. Lopes, D. M. *et al.* Glymphatic inhibition exacerbates tau propagation in an Alzheimer's disease model. *Alz Res Therapy* **16**, 71 (2024).

36. Buccellato, F. R., D'Anca, M., Serpente, M., Arighi, A. & Galimberti, D. The Role of Glymphatic System in Alzheimer's and Parkinson's Disease Pathogenesis. *Biomedicines* **10**, 2261 (2022).

37. Arighi, A. *et al.* Aquaporin-4 cerebrospinal fluid levels are higher in neurodegenerative dementia: looking at glymphatic system dysregulation. *Alz Res Therapy* **14**, 135 (2022).

38. Sacchi, L. *et al.* Association between enlarged perivascular spaces and cerebrospinal fluid aquaporin-4 and tau levels: report from a memory clinic. *Front. Aging Neurosci.* **15**, 1191714 (2023).

39. Wardlaw, J. M. *et al.* Perivascular spaces in the brain: anatomy, physiology and pathology. *Nat Rev Neurol* **16**, 137–153 (2020).

40. Duering, M. *et al.* Neuroimaging standards for research into small vessel disease—advances since 2013. *The Lancet Neurology* **22**, 602–618 (2023).

41. Wardlaw, J. M. *et al.* Neuroimaging standards for research into small vessel disease and its contribution to ageing and neurodegeneration. *The Lancet Neurology* **12**, 822–838 (2013).

42. van der Walt, S. *et al.* scikit-image: image processing in Python. *PeerJ* **2**, e453 (2014).

43. Tustison, N. J. *et al.* N4ITK: Improved N3 Bias Correction. *IEEE Trans. Med. Imaging* **29**, 1310–1320 (2010).

44. Frangi, A. F., Niessen, W. J., Vincken, K. L. & Viergever, M. A. Multiscale vessel enhancement filtering. in *Medical Image Computing and Computer-Assisted Intervention — MICCAI'98* (eds. Wells, W. M., Colchester, A. & Delp, S.) vol. 1496 130–137 (Springer Berlin Heidelberg, Berlin, Heidelberg, 1998).

45. Andersson, J. L. R. & Sotiropoulos, S. N. An integrated approach to correction for off-resonance effects and subject movement in diffusion MR imaging. *NeuroImage* **125**, 1063–1078 (2016).

46. Garyfallidis, E. *et al.* Dipy, a library for the analysis of diffusion MRI data. *Front. Neuroinform.* **8**, (2014).

47. Taoka, T. *et al.* Reproducibility of diffusion tensor image analysis along the perivascular space (DTI-ALPS) for evaluating interstitial fluid diffusivity and glymphatic function: CHanges in Alps index on Multiple conditiON acquIsition eXperiment (CHAMONIX) study. *Jpn J Radiol* **40**, 147–158 (2022).

48. Sacchi, L. *et al.* Unravelling the Association Between Amyloid-PET and Cerebrospinal Fluid Biomarkers in the Alzheimer's Disease Spectrum: Who Really Deserves an A+? *JAD* **85**, 1009–1020 (2022).

49. Dubois, B. *et al.* Clinical diagnosis of Alzheimer's disease: recommendations of the International Working Group. *The Lancet Neurology* **20**, 484–496 (2021).

50. Rascovsky, K. *et al.* Sensitivity of revised diagnostic criteria for the behavioural variant of frontotemporal dementia. *Brain* **134**, 2456–2477 (2011).

51. Crutch, S. J. *et al.* Consensus classification of posterior cortical atrophy. *Alzheimer's & Dementia* **13**, 870–884 (2017).

52. McKeith, I. G. *et al.* Diagnosis and management of dementia with Lewy bodies: Fourth consensus report of the DLB Consortium. *Neurology* **89**, 88–100 (2017).

53. Armstrong, M. J. *et al.* Criteria for the diagnosis of corticobasal degeneration. *Neurology* **80**, 496–503 (2013).

54. Gorno-Tempini, M. L. *et al.* Classification of primary progressive aphasia and its variants. *Neurology* **76**, 1006–1014 (2011).

55. Chad, J. A., Pasternak, O., Salat, D. H. & Chen, J. J. Re-examining age-related differences in white matter microstructure with free-water corrected diffusion tensor imaging. *Neurobiology of Aging* **71**, 161–170 (2018).

56. Pasternak, O., Shenton, M. E. & Westin, C.-F. Estimation of Extracellular Volume from Regularized Multi-shell Diffusion MRI. in *Medical Image Computing and Computer-Assisted Intervention – MICCAI 2012* (eds. Ayache, N., Delingette, H., Golland, P. & Mori, K.) vol. 7511 305–312 (Springer Berlin Heidelberg, Berlin, Heidelberg, 2012).

57. Iliff, J. J. *et al.* Impairment of Glymphatic Pathway Function Promotes Tau Pathology after Traumatic Brain Injury. *J. Neurosci.* **34**, 16180–16193 (2014).

58. Ren, Z. *et al.* 'Hit & Run' Model of Closed-Skull Traumatic Brain Injury (TBI) Reveals Complex Patterns of Post-Traumatic

AQP4 Dysregulation. *J Cereb Blood Flow Metab* **33**, 834–845 (2013).

59. Ma, X. *et al.* Diffusion Tensor Imaging Along the Perivascular Space Index in Different Stages of Parkinson's Disease. *Front. Aging Neurosci.* **13**, 773951 (2021).

60. van Veluw, S. J. *et al.* Cerebral amyloid angiopathy severity is linked to dilation of juxtacortical perivascular spaces. *J Cereb Blood Flow Metab* **36**, 576–580 (2016).

61. Roher, A. E. *et al.* Cortical and leptomeningeal cerebrovascular amyloid and white matter pathology in Alzheimer's disease. *Mol Med* **9**, 112–122 (2003).

62. Wang, M.-L., Yu, M.-M., Wei, X.-E., Li, W.-B. & Li, Y.-H. Association of enlarged perivascular spaces with Aβ and tau deposition in cognitively normal older population. *Neurobiology of Aging* **100**, 32–38 (2021).

63. Banerjee, G. *et al.* MRI-visible perivascular space location is associated with Alzheimer's disease independently of amyloid burden. *Brain* **140**, 1107–1116 (2017).

64. Moses, J. *et al.* Perivascular spaces as a marker of disease severity and neurodegeneration in patients with behavioral variant frontotemporal dementia. *Front. Neurosci.* **16**, 1003522 (2022).

65. Benitez, A. *et al.* Greater Diffusion Restriction in White Matter in Preclinical Alzheimer Disease. *Annals of Neurology* **91**, 864–877 (2022).

66. Collij, L. E. *et al.* White matter microstructure disruption in early stage amyloid pathology. *Alz & Dem Diag Ass & Dis Mo* **13**, e12124 (2021).

67. Zhong, J. *et al.* Unlocking the enigma: unraveling multiple cognitive dysfunction linked to glymphatic impairment in early Alzheimer's disease. *Front. Neurosci.* **17**, 1222857 (2023).

68. Steward, C. E. *et al.* Assessment of the DTI-ALPS Parameter Along the Perivascular Space in Older Adults at Risk of Dementia. *Journal of Neuroimaging* **31**, 569–578 (2021).

69. Zhang, X. *et al.* Glymphatic system impairment in Alzheimer's disease: associations with perivascular space volume and cognitive function. *Eur Radiol* (2023) doi:10.1007/s00330-023-10122-3.

70. Huang, S. *et al.* Glymphatic system dysfunction predicts amyloid deposition, neurodegeneration, and clinical progression in Alzheimer's disease. *Alzheimer's & Dementia* **20**, 3251–3269 (2024).

71. Hsu, J. *et al.* MAGNETIC RESONANCE Images Implicate That Glymphatic Alterations Mediate Cognitive Dysfunction in ALZHEIMER DISEASE. *Annals of Neurology* **93**, 164–174 (2023).

72. Song, H. *et al.* Structural network efficiency mediates the association between glymphatic function and cognition in mild VCI: a DTI-ALPS study. *Front. Aging Neurosci.* **14**, 974114 (2022).

73. Siow, T. Y. *et al.* Association of Sleep, Neuropsychological Performance, and Gray Matter Volume With Glymphatic Function in Community-Dwelling Older Adults. *Neurology* **98**, e829–e838 (2022).

74. Taoka, T. *et al.* Diffusion-weighted image analysis along the perivascular space (DWI–ALPS) for evaluating interstitial fluid status: age dependence in normal subjects. *Jpn J Radiol* **40**, 894–902 (2022).

75. Naganawa, S., Nakane, T., Kawai, H. & Taoka, T. Age Dependence of Gadolinium Leakage from the Cortical Veins into the Cerebrospinal Fluid Assessed with Whole Brain 3D-real Inversion Recovery MR Imaging. *MRMS* **18**, 163–169 (2019).

76. Harrison, I. F. *et al.* Impaired glymphatic function and clearance of tau in an Alzheimer's disease model. *Brain* **143**, 2576–2593 (2020).

77. Peng, W. *et al.* Suppression of glymphatic fluid transport in a mouse model of Alzheimer's disease. *Neurobiology of Disease* **93**, 215–225 (2016).

78. Matsushita, S. *et al.* The Association of Metabolic Brain MRI , Amyloid PET , and Clinical Factors: A Study of Alzheimer's Disease and Normal Controls From the Open Access Series of Imaging Studies Dataset. *Magnetic Resonance Imaging* jmri.28892 (2023) doi:10.1002/jmri.28892.

79. Ringstad, G. Glymphatic imaging: a critical look at the DTI-ALPS index. *Neuroradiology* **66**, 157–160 (2024).

80. Sapkota, D. *et al. Aqp4* stop codon readthrough facilitates amyloid-β clearance from the brain. *Brain* **145**, 2982–2990 (2022).

81. Rainey-Smith, S. R. *et al.* Genetic variation in Aquaporin-4 moderates the relationship between sleep and brain Aβ-amyloid burden. *Transl Psychiatry* **8**, 47 (2018).

82. Shams, S. *et al.* Topography and Determinants of Magnetic Resonance Imaging (MRI)-Visible Perivascular Spaces in a Large Memory Clinic Cohort. *JAHA* **6**, e006279 (2017).

83. Planche, V. *et al.* Structural progression of Alzheimer's disease over decades: the MRI staging scheme. *Brain Communications* **4**, fcac109 (2022).

84. Jack, C. R. *et al.* Tracking pathophysiological processes in Alzheimer's disease: an updated hypothetical model of dynamic biomarkers. *The Lancet Neurology* **12**, 207–216 (2013).

85. Alzheimer's disease Neuroimaging Initiative1 *et al.* An MRI Brain Atrophy and Lesion Index to Assess the Progression of Structural Changes in Alzheimer's Disease, Mild Cognitive Impairment, and Normal Aging: A Follow-Up Study. *JAD* **26**, 359–367 (2011).

86. Pettigrew, C. *et al.* Alzheimer's disease genetic risk and cognitive reserve in relationship to long-term cognitive trajectories among cognitively normal individuals. *Alz Res Therapy* **15**, 66 (2023).

87. Zhu, W. *et al.* The protective impact of education on brain structure and function in Alzheimer's disease. *BMC Neurol* **21**, 423 (2021).

88. Scollard, P. *et al.* Ceiling effects and differential measurement precision across calibrated cognitive scores in the Framingham Study. *Neuropsychology* **37**, 383–397 (2023).

89. Franco-Marina, F. *et al.* The Mini-mental State Examination revisited: ceiling and floor effects after score adjustment for educational level in an aging Mexican population. *Int. Psychogeriatr.* **22**, 72–81 (2010).

90. Himali, J. J. *et al.* Association Between Slow-Wave Sleep Loss and Incident Dementia. *JAMA Neurol* **80**, 1326 (2023).

91. Xie, L. *et al.* Higher intracranial arterial pulsatility is associated with presumed imaging markers of the glymphatic system: An explorative study. *NeuroImage* **288**, 120524 (2024).

92. Mohaupt, P., Vialaret, J., Hirtz, C. & Lehmann, S. Readthrough isoform of aquaporin-4 (AQP4) as a therapeutic target for Alzheimer's disease and other proteinopathies. *Alz Res Therapy* **15**, 170 (2023).

93. Murdock, M. H. *et al.* Multisensory gamma stimulation promotes glymphatic clearance of amyloid. *Nature* **627**, 149–156 (2024).